Observation of long-lived oblique excitons in GaN-AlGaN multiple quantum wells

B. Gil, P. Lefebvre, J. Allègre, and H. Mathieu
CNRS, Groupe d'Etude des Semiconducteurs, Université de Montpellier II, Case Courrier 074, 34095 Montpellier Cedex 5, France

N. Grandjean, M. Leroux, and J. Massies
CNRS, Centre de Recherche sur l' Hétéro-Epitaxie et ses Applications, Rue B. Grégory, 06560 Valbonne, France

P. Bigenwald and P. Christol
Laboratoire de Physique des Matériaux, Université d' Avignon, 33 Rue Louis Pasteur, 84000 Avignon, France
(Received 17 August 1998)

The 2-K recombination dynamics of coupled GaN-AlGaN multiple quantum wells reveals a composite nature in terms of the joint contributions of short-lived direct excitons and long-lived oblique ones. The possibility to observe these oblique excitons, which produce a unusual blueshift of the photoluminescence at long decay times is found to be in straightforward correlation with the presence of internal electric fields together with the existence of a slight disorder at the monolayer scale. [S0163-1829(99)09815-X]

Group III nitride semiconductor compounds are currently emerging as basic materials for developing the electronic[1] and optoelectronic[2] applications of the years to come. Alloyed with arsenic, or phosphorus, they can cover the far infrared to the near ultraviolet regions of the spectrum. In addition, although they naturally grow in the wurtzite phase [α-XN], they can be forced to grow under the metastable zinc-blende phase[3] (β-XN). The wurtzite phase may have some drawbacks, in particular if (DX) centers do not exist[4] in the zinc-blende material, but it has also some unique potentialities. The rest of this paper is devoted to such particular properties of III nitrides in the wurtzite phase. These properties essentially result from the low symmetry: recent theoretical calculations predict large built-in electric fields due to the difference of spontaneous polarizations between two different wurtzite crystals, or/and at the wurtzite-air interface.[5] This has serious implications in the area of quantum wells (QW's): the heterointerfaces are not equivalent, and therefore GaN-AlGaN QW's are naturally grown with an internal electric field.[6] In contrast with more classical systems like GaAs-AlGaAs QW's grown along the [001] direction, the usual macroscopic mirror parity is broken. Consequently, the built-in electric field separates the maxima of the electron and hole wave functions to each side of the QW. Moreover, since the III nitrides used are lattice mismatched to each other, the overall electric field is also a result of piezoelectric polarizations. This effect can either counterbalance or reinforce the effect of the spontaneous polarization, depending on the magnitude and sign of the strain in the different layers.[7] Comprehension of these combined effects on the physical properties of III-nitride QW's is really an issue. In a previous paper,[8] we have reported experimental results showing the joint contributions of both the spontaneous and piezoelectric polarizations in a series of GaN-GaAlN QW's grown by molecular beam epitaxy (MBE). The layer thicknesses and the aluminum composition in the barriers were obtained from reflection high-energy electron diffraction oscillations. X-ray diffraction measurements allowed us to measure the on-axis and in-plane values of the lattice parameters. We have demonstrated the control of the QW thickness with a one-monolayer (ML) accuracy by growing samples containing sequences of GaN wells with variable widths, e.g., with $(4n-1)$ or $(4n+1)$ GaN ML's (with $n=1,2,\ldots$). In these samples, we have observed[9] a nice monotonous dependence of the transition energies versus well width, that clearly evidenced the reliability of our growth procedure and the presence of an electric field of 450 kV/cm in the wells. The interfacial roughness of the layers was also analyzed, since 2-K photoluminescence (PL) spectra are dominated by the radiative recombination of excitons bound to regions where the wells slightly exceed their average width.[8] Time-resolved PL experiments on these samples have convinced us that large built-in electric fields exist not only in GaN wells but also in the narrow (5 nm) GaAlN barriers. The latter fields were found responsible for the efficient nonradiative carrier transfers between the wells, from the narrowest one towards the largest one and, eventually, towards the GaN buffer. These findings were consistent with the theoretical prediction[5–7] that the electric field in such multilayered samples is a function of both spontaneous and piezoelectric polarizations of the materials. The model of Refs. 5–7 also yields and interesting prediction for III-nitride periodic multiquantum wells and superlattices: the potential increase along the growth axis of the GaN well is compensated by an equivalent potential drop across the barriers, so that the overall potential pattern is ''flat.''

In this paper, we focus on the recombination dynamics in such a GaN-$Al_{0.11}Ga_{0.89}N$ multiple quantum well (MQW). The aim of this paper is to compare this dynamics with previous observations in single QW's and in multi-QW's with wells of different widths. Our results lead us to address the effects of built-in electric fields—and of distributed layer widths—on ''intrawell'' and ''interwell'' excitonic transitions. Indeed, we observe the coexistence of short-lived excitons, made of electrons and holes confined in a same well, with long-lived excitons made of electrons and holes confined in adjacent wells. This observation is another evidence of electric fields through the whole MQW structure. Indeed,

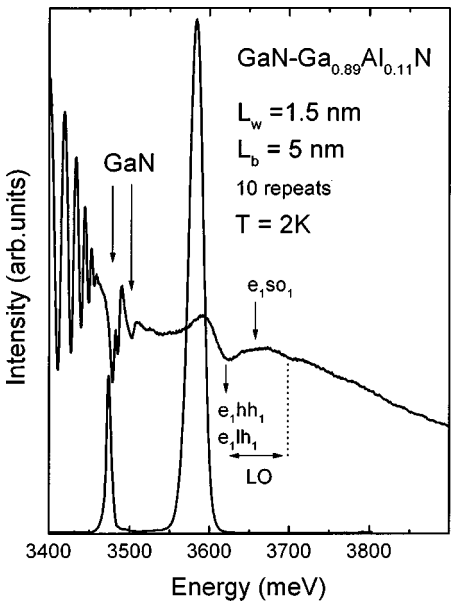

FIG. 1. 2-K *cw* photoluminescence and reflectance spectra for the multiple quantum-well structure.

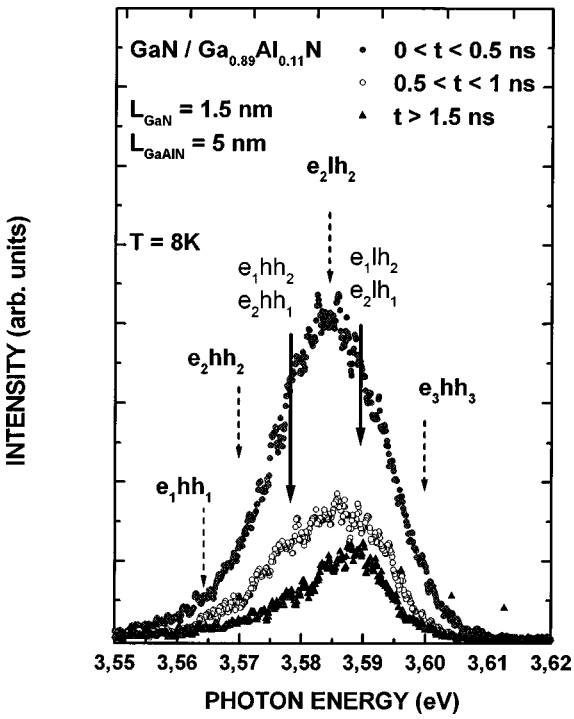

FIG. 2. 8-K photoluminescence spectra taken at various delays after the laser pulse (see text for details). The labeling of the transitions corresponds with the envelope function calculations described in the text.

our results are in good agreement with envelope-function calculations of exciton energies and oscillator strengths, only if the above-mentioned ''flat'' overall potential is included.

The sample was grown by MBE on a 2-μm thick GaN buffer layer, itself being deposited on the *c* face of a sapphire substrate. The average width of the ten GaN wells is 6 ML (1 ML equals 0.26 nm), and the average width of the $Al_{0.11}Ga_{0.89}N$ barriers is 20 ML. The in-plane lattice parameter of the GaN is $a_{GaN}=3.1892$ Å at 300 K. An x-ray diffraction mapping has shown that the AlGaN layers are lattice matched onto the GaN, along the growth plane (the 2 K lattice parameters can be estimated following Skromme's approach[12]).

Figure 1 (bottom) displays the *cw* PL spectrum taken at $T=2$ K by using the 325-nm radiation of a HeCd laser. Two PL lines are observed at 3470 and 3584 meV, respectively. The low-energy line corresponds to the PL from the GaN buffer layer. At higher energy, the efficient recombination line is the signature of the MQW. The full widths at half maximum are 7 and 20 meV, respectively. The reflectance spectrum of the sample is also shown in Fig. 1 (top). The three features of the *A*, *B*, and *C* free excitons in GaN are detected at 3476, 3484, and 3502 meV. These values are close to the values expected for slightly strained or unstrained GaN.[13,14] The 6 meV difference between the low-energy PL line and the low-energy reflectance feature is simply the binding energy of the neutral-donor-bound exciton that dominates, as often observed,[15] the PL spectrum of the GaN buffer. For the MQW, there is a substantial Stokes shift between the strong PL peak and the reflectance feature at 3612 meV. This is not a surprise: in our previous studies[8] on MQW's with wells of different widths, the PL corresponded to the recombination of excitons in zones where the well width exceeds its average value by 2 ML. The relative proportion of these localization zones is rather small: we have shown, indeed, that thermal detrapping of excitons occurs below 100 K and that the reflectance feature always corresponds to the average thickness.[8]

In the present MQW sample the localization behavior is much more complicated, as addressed below via time-resolved spectroscopy. The reflectance feature in the 3612-meV region is composite: envelope function calculations detailed below show that both contributions of Γ_9 and Γ_7 confined hole states contribute to this reflectance feature, but are not resolved. The same calculations allow us to assign the smooth reflectance variation near 3.65 eV to the contribution of the confined Γ_7 spin-orbit split-off hole. It is interesting to discuss another change in reflectance observed near 3704 meV, i.e., one LO phonon energy above the main reflectance feature. This line is attributed to a hot exciton. This means that a photon having the energy equal to the exciton creation energy plus the phonon energy is absorbed, producing an exciton and emitting a LO phonon simultaneously.

The experimental setup for time-resolved photoluminescence has been described elsewhere:[10] 2-ps laser pulses with $\lambda\sim 270$ nm excite the sample at a repetition frequency of 82 MHz. The PL signal is dispersed through a spectrometer and detected by a streak camera giving an overall temporal resolution of $\sim$5 ps, after the standard deconvolution procedures.

We begin by the low-temperature recombination dynamics. We have recorded the PL spectra at various delays after the excitation pulse (Fig. 2). For small delays, the PL lineshape is very similar to the PL lineshape obtained by the *cw* excitation, shown in Fig. 1. For larger times, there is a significant distortion of the PL lineshape, resulting in an overall blueshift, for sufficient delays. This quite unusual observation implies a complicated spectral dependence of the recombination time and, most probably, the coexistence of several radiative channels in the same spectral range, with no fast connection between them. Otherwise, we should have ob-

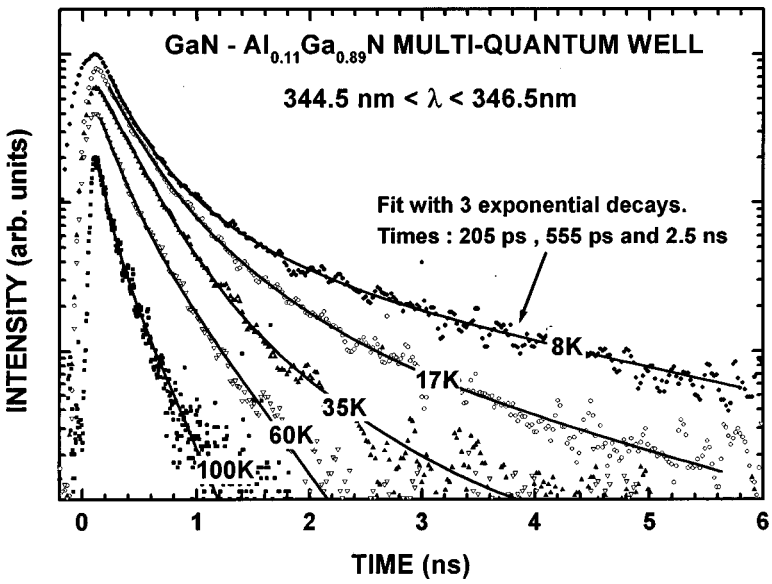

FIG. 3. Multiexponential decays, at various temperatures, of the PL integrated spectrally over the entire emission line of the MQW, i.e., between 3577 and 3598 meV.

served an overall redshift, as we did for a *single* GaN-GaAlN QW, recently.[11] The latter result was interpreted, in fact, by the relaxation of an initial effective blueshift induced both by band-filling effects and by the screening of the built-in electric field.[16]

For this MQW we have analyzed the spectral dependence of the dynamics of the PL decay. In no region of the spectrum is the decay monoexponential. Instead, we can select two or three dynamical regimes, which are present with a varying weighting across the PL line. Dashed arrows in Fig. 2 show the regions where rather fast decays are dominant; the decay time there is of the order of 200–250 ps typically, although slower contributions are also present. Bold arrows show the regions where the latter slow processes dominate; their decay time lies in the range of 2–3 ns, although contributions with even larger times must be included for a satisfactory multiexponential fit to experimental data. Again, this complex behavior is totally at variance from what is expected from excitons localized at well-width fluctuations in a quantum well: the larger the well there, the stronger the localization and the larger the radiative lifetime.[17] Then, the decay should be rather exponential, with time constants decreasing monotonically with emission wavelengths.[18]

The above situation only accounts for spatially direct excitons, with electrons and holes localized in the same QW. But we should remember that, in MQW structures, spatially indirect localized exciton states can exist if the in-plane localization energies of electrons and holes exceed the corresponding miniband widths. This is is exactly the case in our sample. Moreover, the observation of spatially indirect excitons should be favored by electric fields in GaN wells: the latter tend to push the electron wave function of one well towards one interface of this well, whereas the field also pushes the hole wave function of the next well in the opposite direction, i.e., towards the electron of the previous well. These indirect excitons live longer than direct ones because of smaller electron-hole overlap. Obviously, a narrow barrier favors the recombination probability of these indirect excitons. This is why we did not observe such long-lived contributions in a previous paper[10] on MQW's with 10-nm wide barriers. Moreover, interwell excitons may have higher energies than direct excitons for two reasons: first, the overall ''flat'' potential profile causes the band-to-band energies to be almost the same for intrawell and interwell transitions. Second, the exciton binding energy is smaller for an indirect state.

Nevertheless, the apparent blueshift at large delays could not be observed without localization effects. The observed indirect excitons involve an electron and a hole localized in regions of the layer plane where their respective wells are wider than the average width. This localization avoids that the carrier of interest recombine efficiently with another hole or electron within its ''own'' well. This scenario also implies a variety of in-plane electron-hole configurations in terms of their mutual distance, inducing a variety of energies and decay times for these processes.

We thus explain our observations by the superimposition, in the same spectral range, of a variety of recombination processes, which we may class into two families: the direct, intrawell excitons, with small decay times, and the indirect, interwell excitons, with large decay times. The analysis of the overall PL decay versus temperature T, comes in support of this interpretation. Indeed, spatially indirect excitons are expected to dissociate more easily than direct ones, when increasing T. This is exactly what is shown in Fig. 3. At $T = 8\,\mathrm{K}$, the decay is multiexponential: three exponentials have been used for the fitting shown by the solid line. The time constants are 205 ps, 0.55 and 2.50 ns, respectively. When T is increased, the time constants remain almost identical. More precisely, the two faster components become slightly slower and the slowest component becomes slightly faster, up to 60 K. But the weights of the two slower contributions rapidly vanish, so that the fastest component widely dominates the decay. Above 60 K, all time constants are reduced, due to enhanced nonradiative effects. At 100 K, the decay is almost monoexponential, with a time constant of 85 ps.

We wish to enforce our demonstration by giving an example of what probably occurs in this sample, through a

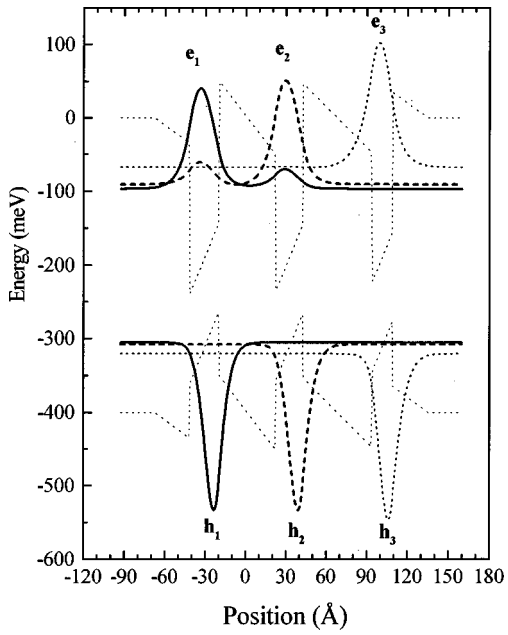

FIG. 4. Typical electron (top) and heavy-hole (bottom) densities of probability together with the potential lineups.

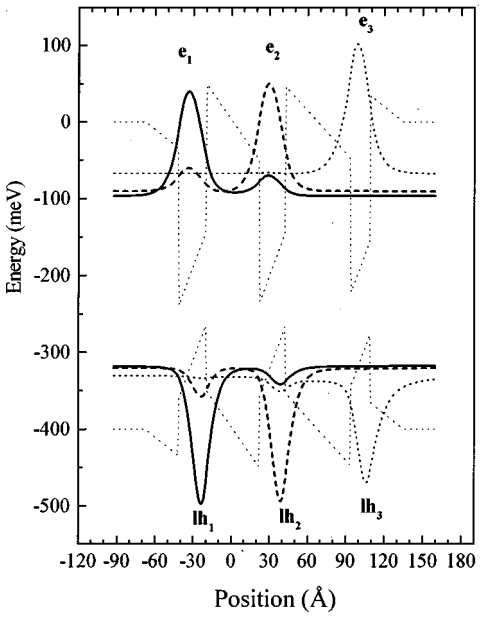

FIG. 5. The analog of Fig. 3 for electron (top) and light-hole-hole (bottom) densities of probability.

reasonable model. We note that many material parameters are still poorly known and that the quantitative analysis of built-in electric fields in nitride heterostructures is only at its beginning. Thus, the envelope-function calculations shown below should be taken as an illustration rather than as a real fitting such as those we could do for more usual quantum wells. We recall here that we found a residual field of 450 kV/cm in similar samples[8] with wells of varying widths. We have thus retained this value here, although it may be slightly different, and we have compensated it by a field of opposite sign in the barriers adapted so that the overall ''flat'' potential situation is obtained. The resulting potential profile is sketched in Fig. 4: for simplicity, we have considered three wells only. A transfer matrix algorithm was used to compute the transition energies. The calculations for light holes are more complicated than for heavy holes: a two-band envelope function is required,[19] since light-hole and spin-orbit split-off hole states have the same Γ_7 symmetry. The total wave function is expanded along the two Bloch waves $\Gamma_7^1 = 1/\sqrt{2}|x + iy\rangle\downarrow$ and $\Gamma_7^2 = |z\rangle\uparrow$. We will not detail this computation, but the squares of the coefficients of Γ_7^1 are given for the states of interest in Fig. 5. They differ from the probability densities calculated for heavy holes.

The envelope functions in Figs. 4 and 5 correspond to the layer widths, which provided the best agreement with our experimental transition energies. These layer widths produce an asymmetrical system where a well having the average width (6 ML) is neighbored by two wider wells. This 6-ML wide well (well 3 with our notations) is adjacent to a second one having a width of 8 ML (well 2) itself being also adjacent to a wider well (8.5 ML) on the left-hand side (well 1). Interestingly, due to the presence of electric fields, *and* of some disorder in well widths, the electron-envelope function, shown in Figs. 4 and 5, slightly spreads in the adjacent well. Such a tunneling *does not* occur for the heavy hole, mainly because of its very large effective mass.

We have plotted in Fig. 6 the inverse square of the electron-hole envelope-function overlap integrals, for each of the intrawell or interwell transitions, versus the excitonic transition energies. This quantity is proportional to the radiative lifetime of the corresponding excitons. The transitions are labeled $e_i l(h) h_j$ when electron and hole densities of probabilities are dominantly peaking in wells i and j, respectively. The excitonic interaction was computed in the context of a two-parameter variational approach. Examples of calculated exciton-binding energies are as follows. For intrawell excitons, we found: $e_1hh_1 = 34.4$ meV, $e_2hh_2 = 33.6$ meV, $e_3hh_3 = 39.7$ meV, $e_1lh_1 = 30.9$ meV, and $e_2lh_2 = 30.4$ meV. For interwell excitons, we found: $e_1hh_2 = 17.3$ meV, $e_2hh_1 = 18.8$ meV, $e_1lh_2 = 15.4$ meV, and $e_2lh_1 = 20.7$ meV. In Fig. 6, we note two bands at 3585 and

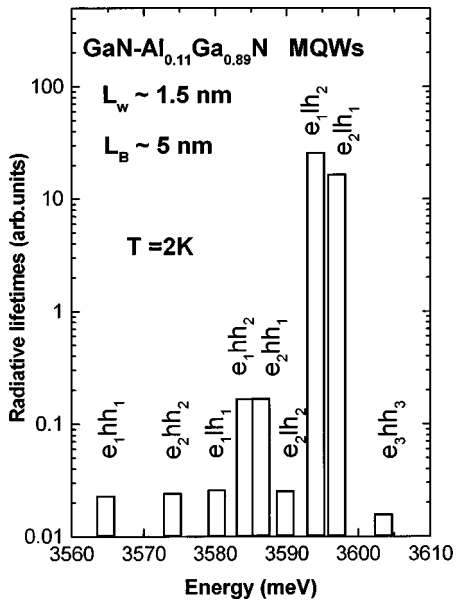

FIG. 6. Plot of the radiative lifetimes as a function of the excitonic transition energies.

3595 meV, respectively, which correspond to long decay times and faster transitions at lower and higher energies. We have performed similar calculations in the absence of fluctuations of well widths. In this case, the squares of envelope functions e_1 and e_2 become almost identical and the electron-hole overlaps do not exhibit the same trend as above, i.e., with small overlaps for oblique excitons. We thus conclude that the distribution of lifetimes in our photoluminescence bands essentially arises from the distribution of well widths, which favors the formation of both intrawell and interwell excitons. This kind of effect had already been observed in previous studies, for monolayer fluctuations in symmetrical and asymmetrical double-quantum wells.[20] Our variational calculation yields quite correct exciton energies and a reasonable order of magnitude for the change of exciton lifetimes across the PL line. Note that the lifetime calculation does not include the in-plane localization of excitons, which multiplies the lifetime by a factor of $\sim$200 (see Ref. 10).

Again, we wish to stress that the above calculation is an illustration of the kind of effects that occur in our MQW sample. In particular, the existence of long-lived excitons at higher energy than short-lived ones is clearly a consequence of specific potential profiles (electric fields), of disorder effects (widths fluctuations) and of different binding energies for direct and indirect excitons. In practice, the distribution of decay times across the PL line is also a result of the thermalization of individual carriers, which favors the observation of lower-energy transitions, and a result of the statistical distribution of the various configurations. We have checked that other variations of layer widths would not yield completely different results. We kept the same values for electric fields and performed the same calculations for a variety of situations, involving wells having widths from 6 to 9 ML and barriers with monolayer variations around the average width of 5 nm. In particular, regarding the situation detailed above, we have tried permutations of the different wells. The overall results can be summarized in the following way: we find that short-lived, intrawell excitons cover an energy range between 3585 and 3625 meV, whereas interwell excitons occupy mainly two energy ranges, i.e., 3595–3605 meV and 3615–3620 meV. Considering the simplicity of the model and the uncertainty on several parameters, this result is satisfactory because it explains the multiexponential decay and the overall effective blueshift at large delays.

In conclusion, we have evidenced the existence of long-lived oblique excitons in GaN-AlGaN multiple quantum wells. We have shown that such excitons are observed due to the distribution of well widths and to built-in electric fields in the well and barrier layers. The physics of these quantum wells is currently living its infancy and it is clear that utilization of these effects together with external biasing is a key issue in the area of optical switches since the absorption of light is very efficient in nitrides.

We are grateful to M. Laügt for the XRD experiments. B.G. acknowledges A. V. Kavokine for enlightening discussions.

[1] J. Y. Duboz and M. Asif Khan, in *Group III Nitride Semiconductor Compounds*, edited by B. Gil (Clarendon, Oxford, 1998).
[2] S. Nakamura and G. Fasol, *The Blue Laser Diode* (Springer, Berlin, 1997).
[3] For a review, see, for instance, O. Brandt, in *Group III Nitride Semiconductor Compounds* (Ref. 1).
[4] C. Van de Walle, Phys. Rev. B **57**, R2033 (1998).
[5] F. Bernardini, V. Fiorentini, and D. Vanderbilt, Phys. Rev. B **56**, R10 024 (1997).
[6] F. Bernardini and V. Fiorentini, Phys. Rev. B **57**, R9427 (1998).
[7] F. Bernardini and V. Fiorentini, Phys. Rev. B **58**, 15 292 (1998).
[8] M. Leroux, N. Grandjean, M. Laügt, J. Massies, B. Gil, P. Lefebvre, and P. Bigenwald, Phys. Rev. B **58**, 13 371 (1998).
[9] N. Grandjean and J. Massies, Appl. Phys. Lett. **73**, 1260 (1998).
[10] P. Lefebvre, J. Allègre, B. Gil, A. Kavokine, H. Mathieu, W. Kim, A. Salvador, A. Botchkarev, and H. Morkoc, Phys. Rev. B **57**, R9447 (1998).
[11] P. Lefebvre, J. Allègre, B. Gil, H. Mathieu, N. Grandjean, M. Leroux, and J. Massies (unpublished).
[12] B. J. Skromme, Mater. Sci. Eng., B **50**, 117 (1997).
[13] B. Gil, in *Semiconductors and Semimetals*, edited by J. I. Pankove and T. D. Moutsakas (Academic, New York, 1998), Vol. 57, pp. 209–274.
[14] H. Teisseyre, G. Nowak, M. Leszczynski, I. Grzegory, M. Bockowski, S. Krukowski, S. Porowski, M. Mayer, A. Pelzmann, Markus Kamp, K. J. Ebeling, and G. Karczewski, MRS Internet J. Nitride Semicond. Res. **1**, 13 (1996).
[15] M. Leroux, B. Beaumont, N. Grandjean, P. Lorenzini, S. Haffouz, P. Vénnégues, J. Massies, and P. Gibart, Mater. Sci. Eng., B **50**, 97 (1997).
[16] P. Boring, B. Gil, and K. J. Moore, Phys. Rev. Lett. **71**, 1875 (1993).
[17] A. V. Kavokine, J. Phys. IV **3**, 79 (1993).
[18] M. Colocci, M. Gurioli, and J. Martinez-Pastor, J. Phys. IV **3**, 3 (1993).
[19] P. Bigenwald, P. Christol, L. Konczewicz, P. Testud, and B. Gil, Mater. Sci. Eng., B **50**, 208 (1997), and references therein.
[20] P. Bonnel, P. Lefebvre, B. Gil, H. Mathieu, C. Deparis, J. Massies, G. Neu, and Y. Chen, Phys. Rev. B **42**, 3435 (1990).